

Theory of Molecular Scattering from and Photochemistry at Ice Surfaces

G. J. Kroes¹ and S. Andersson^{1,2}

¹Leiden Institute of Chemistry, Gorlaeus Laboratories, Leiden University,
P.O. Box 9502, 2300 RA Leiden, The Netherlands
email: g.j.kroes@chem.leidenuniv.nl

²Leiden Observatory, Leiden University, P.O. Box 9513, 2300 RA Leiden, The Netherlands

Abstract. The classical trajectory methodology for studying scattering of ions, atoms, or molecules from ice surfaces, and photodissociation of water at or in the surface of ice, is presented. The forces between the collider and the water molecules, or between the fragments of a dissociating molecule and the surrounding water molecules, are based on pair potentials taken either from *ab initio* calculations or derived empirically. Dynamical observables like sticking probabilities and kinetic energy distributions of desorbing photo-fragments are computed by solving Newton's equations of motion, starting from representative initial conditions. Four studies with relevance to astrochemistry are considered: the sticking of H atoms to ice Ih, the sticking of CO to ice Ih and ice I_a, the sticking of protons to ice Ih, and the photodissociation of water in ice Ih and ice I_a, also with a view to the subsequent chemistry of the H- and OH-products with co-adsorbed molecules. Where possible, the theoretical results are compared with experiments.

Keywords. astrochemistry — ISM: molecules — methods: numerical — molecular processes

1. Introduction

The formation of molecules in the interstellar medium (ISM) can proceed through several classes of reactions (van Dishoeck 1998). An important class consists of surface reactions, which take place on dust particles. In dense clouds, these dust particles, can be covered by icy mantles (Ehrenfreund & Schutte 2000). The ice can consist of H₂O molecules, but molecules like CO, CO₂, NH₃, and CH₄ may also be present. The icy mantles are generally believed to have an amorphous structure (Hagen *et al.* 1981). However, crystalline ice (ice Ih) can also be relevant to astrochemistry. For instance, amorphous ice (ice I_a) deposited on amorphous silicate particles can be phase transformed to crystalline ice at temperatures close to 110 K (Maldoni *et al.* 1999). On dust particles in the ISM, this temperature can be achieved through the impact of cosmic rays. In this paper, we will therefore consider processes occurring on both amorphous and crystalline pure water ice.

An important example of a surface reaction taking place on dust particles is the formation of molecular hydrogen, the most abundant molecule in the ISM. It is generally assumed that the H₂ in the ISM is formed through surface reactions occurring on grains (Hollenbach & Salpeter 1971; Herbst 1995). Because the mechanism of hydrogen recombination always involves the trapping of at least one hydrogen atom at the surface prior to reaction, the study of trapping (sticking) of H to ice is relevant to the astrochemistry of dense clouds. We will present results (Al-Halabi *et al.* 2002) of calculations on the trapping of H on ice Ih, and compare these with calculations as well as experiments on the trapping of H on ice I_a.

Solid CO has been observed along many lines of sight towards the dense regions in the ISM, the Galactic center, and high- and low-mass young stellar objects (Tanaka *et al.* 1994; Pontoppidan *et al.* 2003). Observations suggest that CO resides in two distinct environments; *i.e.*, in van der Waals bonded ice (also called apolar ice or H₂O-poor ice), and in hydrogen bonded ice (also called polar ice or H₂O-rich ice). One question concerning the hydrogen bonded ice is related to the mixing of CO and H₂O: does an intimate mixture form, or is CO present in multilayer form on the surface of H₂O ice? Clever experiments using coadsorbates which either bond or do not bond to surface dangling OH-groups of H₂O ice (Devlin 1992; Graham *et al.* 1999) strongly suggest that intimately mixed ice should exhibit a 2152 cm⁻¹ feature in the infrared due to the interaction of CO with dangling OH bonds, while a 2139 cm⁻¹ feature should be due to CO-CO interactions in solid CO ice, or interactions of CO with “bonded OH”. These experiments also suggest that the dangling OH-bonds should be the preferred adsorption sites of isolated CO-molecules adsorbed to H₂O ice. Molecular dynamics (MD) calculations employing accurate pair potentials can provide support for the above interpretation of laboratory experiments and observations, and yield insight into the dynamics of trapping of CO on ice. Such calculations (Al-Halabi *et al.* 2003; Al-Halabi, van Dishoeck, & Kroes 2004; Al-Halabi *et al.* 2004) are also reported here.

Interactions of protons with water ice are also relevant to astrochemistry. Cosmic rays (CRs) consist predominantly of high-energy protons. The CR-ice interaction is the predominant agent leading to mass loss of water-ice grains (Mukai & Schwehm 1981). Impact of CRs on mixed ices can promote the formation of molecules like carbonic acid (H₂CO₃) (Gerakines *et al.* 2000) and amino acids (Kobayashi *et al.* 1995). We will therefore also present new, surprising results for the sticking of H⁺ ions to ice Ih (Cabrera Sanfelix *et al.* 2005). The results are for a range of energies (0.05–4.0 eV) which is much lower than the kinetic energy of CR protons. The results are nevertheless of interest. First, they show that a spin-off of research on systems of astrochemical interest may be that new discoveries in chemical physics are made, although some of these discoveries might apply to conditions that are not of direct interest to astrochemistry. Second, we expect that many of the conclusions derived from our study (Cabrera Sanfelix *et al.* 2005) should also be applicable to low-energy collisions of H⁺-containing molecular ions (such as H₃⁺) with ice.

Photodissociation of water in ice, which can be induced by UV light of energy exceeding 7.6 eV (Kobayashi 1983), is also of interest to astrochemistry. The products of the reaction (H and OH, and possibly other products as well) can go on to react with co-adsorbed or co-absorbed molecules. It has been postulated that CO₂ could be formed in this way, *i.e.*, by reaction of OH with CO present on or in H₂O rich ice (Allamandola *et al.* 1988), and experiments on UV irradiation of mixed CO:H₂O ice have indeed shown efficient CO₂ formation (Watanabe & Kouchi 2002). We here present results on the dynamics of photodissociation of H₂O in ice, with much attention paid to the dynamics of the H and OH fragments, also with a view to their possible subsequent chemistry with co-adsorbates (Andersson *et al.* 2005; Andersson *et al.*, in prep.) The calculations to be presented may be viewed as a first step in the modeling of photoinitiated reactions of products of water photolysis with co-adsorbed molecules.

We first discuss the molecular dynamics (MD) method we use in our calculations on sticking and photodissociation of H₂O in ice, in § 2. Results of our MD calculations are presented in § 3, for H + ice Ih (§ 3.1), CO + ice Ih and ice I_a (§ 3.2), H⁺ + ice Ih (§ 3.3), and photodissociation of water in ice Ih and I_a (3.4). We conclude with a summary (§ 4).

2. Method

In this section, we discuss how an MD simulation of molecular processes on or in ice is performed. Whichever problem is studied, such simulations always share common features. First of all, the initial state of the system is prepared, according to the problem of interest. This includes the setting up of a dynamic ice surface (§ 2.1), and the choice of other initial conditions, such as the selection of the coordinates and momenta of the collider (for calculations on sticking) (§ 2.4). Subsequently, Newton's equations of motion have to be solved for a long enough period of time, and relevant observables have to be extracted (§ 2.2). This can only be done if the forces between the molecules are defined, which we do through pair potentials (§ 2.3).

2.1. The Ice Surface

The crystalline and amorphous ice surfaces were modeled using the MD method (Allen & Tildesley 1987). Ice Ih is always modeled as proton disordered (see Kroes 1992). The lower part of the ice Ih surface is usually modeled by 2 bilayers of H₂O molecules (120 molecules) which are held fixed. The upper part of the surface is modeled by 4 or 6 bilayers of H₂O molecules (240 or 360 molecules) which are allowed to move according to Newton's equations of motion. The H₂O molecules are modeled as rigid rotors, with only one exception: if the photodissociation of water in ice is modeled, the photoexcited molecule's intramolecular motion following photoexcitation is also modeled in order to follow the dissociation dynamics and to enable the computation of the absorption spectrum. The H₂O molecules are put in a box which is replicated in two directions according to periodic boundary conditions, to create an infinite ice surface. The TIP4P pair potential (Jorgensen *et al.* 1983) is used to model the forces between the water molecules, because its use yields stable ice Ih at the relevant temperatures (Kroes 1992; Karim & Haymet 1988). For ice Ih, the initial ice configuration obeys the famous ice rules (Bernal & Fowler 1933), and has a zero dipole moment (Kroes 1992). The surface temperature (T_s) of interest is imposed on the ice surface through the use of the computational analogue of a thermostat (Berendsen *et al.* 1984). For details and for a more technical discussion of the setting up of a surface of ice Ih, the reader is referred to Kroes (1992).

In Figure 1, top (1a) and side views (1c) of ice Ih are shown, where it is the (0001) basal plane face of ice that is exposed to the vacuum. Ice Ih has a bilayer structure, the bilayers being about 3.5 Å thick. Another important observation is that the water molecules in the upper monolayer can either have one H atom pointing away from the surface (dangling OH), or both H atoms pointing obliquely down to the surface. This has important consequences for adsorption of CO and protons (see § 3).

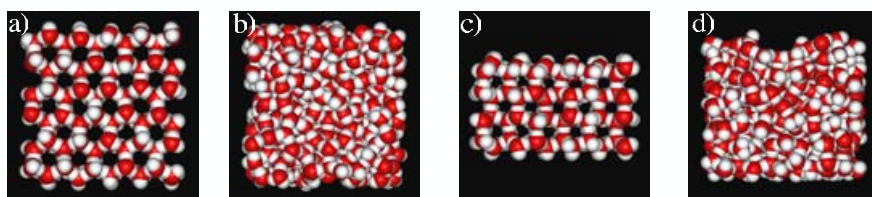


Figure 1. Top views (a and b) and side views (c and d) are shown of simulated ice Ih (a and c) and ice I_a (b and d), at $T_s = 90$ K. In the figures, the dark atoms are the oxygen atoms, and the light atoms the hydrogen atoms.

Interstellar H₂O ice is believed to be predominantly amorphous in structure (Hagen *et al.* 1981). The specific morphology of amorphous ice remains an open

question. The H₂O ice is thought to form through chemical reactions of H and O atoms on dust grains, but it is not known to exactly which structure this would lead. One usually assumes that the structure closely resembles that of ice grown by vapor deposition in the laboratory, known as amorphous solid water (ASW), rather than ice phases formed under high-pressure conditions, such as high-density amorphous (hda) ice, or low-density amorphous (lda) ice (Petrenko & Whitworth 1999; Ehrenfreund *et al.* 2003). We make amorphous ice (Al-Halabi, van Dishoeck, & Kroes 2004; Al-Halabi *et al.* 2004) by first heating hexagonal ice to room temperature, resulting in melting, and subsequent fast cooling (hyperquenching) to the desired temperature, using the computational analogue of a thermostat (Berendsen *et al.* 1984). The calculated average density of our amorphous ice is about 0.93 g/cm³, which is in the range of measured densities (0.85–1.05 g/cm³) of dense amorphous solid water deposited at $T = 22$ K for a wide range of deposition angles (Dohnálek *et al.* 2003). Just as for the case of ice Ih, the surface consists of a box of molecules which is replicated in two directions.

In Figure 1, top (1b) and side views (1d) of the dense ice I_a we made are shown. The amorphous ice completely lacks the regularity seen in ice Ih. The surface of ice I_a is irregular, displaying holes, into which CO can move and interact with many H₂O molecules simultaneously. Most of the water molecules hydrogen bond to 4 neighbouring water molecules, while a substantial fraction hydrogen bond to only 3 neighbouring water molecules (Al-Halabi *et al.* 2004).

2.2. Classical Dynamics and Calculation of Absorption Spectrum

To simulate the dynamics of a collision or photodissociation event, Newton's equations of motion are integrated in time. The integration is started from coordinates and momenta that are representative of the initial conditions (§ 2.4). Sticking probabilities and dynamical quantities related to photodissociation are determined by following the trajectory in time. For instance, to determine a sticking probability (P_s), first an operational definition is made of sticking. A requirement for sticking to occur in the MD is that a trajectory exhibit multiple turning points in the curve showing the molecule-surface distance as a function of time. An additional criterion may be that the final energy of the adsorbed molecule is less than a predefined threshold value. For the actual definition adopted in individual cases, the reader is referred to Al-Halabi *et al.* (2002), Al-Halabi *et al.* (2003), Al-Halabi, van Dishoeck, & Kroes (2004), Al-Halabi *et al.* (2004), and Cabrera Sanfelix *et al.* (2005). The calculation of dynamical quantities associated with photodissociation of H₂O in ice is discussed in Andersson *et al.* (2005) and Andersson *et al.*, in prep.

The absorption spectrum is calculated according to Schinke (1993):

$$\sigma_{tot}^{(i)}(\omega) \propto E_{photon} \int d\tau P_W^i(\tau) \mu_{if}^2 \delta[H_f(\tau) - E_f] \quad (2.1)$$

Here, $P_W^i(\tau)$ is the probability distribution function associated with the initial (*i*) vibrational state of the molecule in its ground electronic state, and $H_f(\tau)$ the Hamilton function in the upper electronic state (*f*). Furthermore, μ_{if} is the transition dipole function, E_i the energy of the initial state, and $E_f = E_i + E_{photon}$. $P_W^i(\tau)$ is calculated from a Wigner (semi-classical) distribution function fitted to the ground state vibrational wave function of the water molecule to be photodissociated, as discussed in van Harreveld *et al.* (2001). The integration is over the entire phase space. The transition dipole moment function was taken from van Harreveld & van Hemert (2000). The spectrum is calculated by determining the energy difference between the excited state potential and the ground state potential for a large number of phase space points, and the absorption spectrum is calculated as the number of times excitation energies occur within an energy

Table 1. Essential features of the pair potentials for the interaction of the collider X with an individual water molecule. Below, R_{min} refers to the distance between a defined atom pair, in the potential minimum geometry.

X	Method of derivation	Potential minimum (kJ mol ⁻¹)	R_{min} (Å)	Atom pair R_{min} refers to	References
CO	HF + MP2	-5.1	2.47	C-H _w	Al-Halabi <i>et al.</i> (2003)
H	UHF + MP4	-0.63	3.4	H-O _w	Al-Halabi <i>et al.</i> (2002) Zhang <i>et al.</i> 1991
H ⁺	empirical	-705	1.04	H ⁺ -O _w	Cabrera Sanfelix <i>et al.</i> (2005) Kozack & Jordan (1992)

interval of a predetermined width. The approach outlined above has been shown to give good agreement between classical and quantum treatments of gas phase photodissociation (Schinke 1993). For more details on how we apply this procedure, see also Andersson *et al.* (2005) and Andersson *et al.*, in prep.

2.3. Pair Potentials

For the integration of the equations of motion, it is necessary to specify the forces that act between the water molecules belonging to the ice, and between the water molecules and the collider (sticking) or between the water molecules and the water molecule that was (or is to be) excited. The potential from which these forces are derived is always based on pair potentials acting between the collider (or the water molecule singled out for photoexcitation) and an H₂O molecule. The total interaction of the collider (or the special water molecule) with the ice surface is then taken as a sum over all (other) H₂O molecules.

The pair potentials used in the calculations on sticking are either taken from *ab initio* calculations or derived empirically. The validity of the pair potential is usually checked by comparison to experimental results. For instance, the CO-H₂O pair potential that was used (Al-Halabi *et al.* 2003; Al-Halabi, van Dishoeck, & Kroes 2004; Al-Halabi *et al.* 2004) was based on *ab initio* HF + MP2 calculations, and the minimum geometry obtained from the pair potential was checked to compare favorably with Fourier transform microwave absorption spectroscopy experiments (Yaron *et al.* 1990). Details on the pair potentials used in the calculations for H, CO, and H⁺ + H₂O can be found in Al-Halabi *et al.* (2002), Al-Halabi *et al.* (2003), and Cabrera Sanfelix *et al.* (2005), respectively. Some essential features of the pair potentials are summarized in Table 1.

In the calculations on photodissociation of water in ice, the potential energy of the water molecule singled out for photoexcitation consists of an intramolecular and an intermolecular part. In the computation of the photoabsorption spectrum, the intramolecular potentials of the photoexcited H₂O molecule in its ground electronic and first excited states are taken from the work of Dobbyn & Knowles (1997).

For the molecule that is photoexcited, the intermolecular interaction with the surrounding water molecules is taken from the TIP3P model (Jorgensen *et al.* 1983), to avoid the complication, arising with the TIP4P model, that the negative charge is not on the (moving) O atom. In the calculation of the absorption spectrum and in the MD calculation on the dynamics following photoexcitation, the excited water molecule interacts with the surrounding water molecules as an excited state water molecule would. In the first potential model we used, charges were put on the O and H atoms of the

excited molecule (Andersson *et al.* 2005) to mimic the dipole moment exhibited by gas phase water in its first excited electronic state (Klein *et al.* 1996). In our second potential model, smaller charges ($-0.2e$ on O and $0.1e$ on H) were used such that the theoretical spectrum was in good agreement with the experimental spectrum (Kobayashi 1983). For a detailed discussion of the pair interaction between excited H_2O and the surrounding H_2O molecules, the reader is referred to Andersson *et al.*, in prep.

2.4. Initial Conditions

The initial coordinates and momenta from which trajectories are started are selected to represent the physical situation of interest, using a Monte Carlo procedure (Porter & Raff 1976). The initial conditions are obtained by equilibrating the ice surface in a separate MD run, after a T_s has been imposed (§ 2.1). For simulating the collision of an atom, ion, or molecule with the surface, the collider's initial momentum is selected according to the collision energy and incidence angle of interest. If the collider is a molecule, its initial orientation is taken at random from uniform distributions of $\cos\theta$ and ϕ , where θ and ϕ are the polar angles of orientation of the molecule's bond axis. The molecule's rotational angular momentum J_c is taken as $J_c = \hbar\sqrt{J(J+1)}$, where J is the molecule's rotational quantum number. The direction of the angular momentum is taken from a random distribution. The collider's impact site on the surface is likewise selected at random.

In the calculations on the photodissociation of water in ice, the initial coordinates and momenta associated with the centre-of-mass motion and rotation of all H_2O molecules are obtained using a separate MD run. The water molecule to be excited is selected to be one of the water molecules present in a given layer of the simulated ice. Its initial intramolecular coordinates and vibrational momenta are selected at random from the probability distribution obtained from a semi-classical wave function – the Wigner distribution (van Harreveld *et al.* 2001). Therefore, the initial phase-space distribution of the dissociating molecule is based on quantum mechanics.

3. Results and Discussion

3.1. $H + \text{Ice}$

The sticking probability (P_s) computed for scattering of atomic hydrogen from ice Ih at normal incidence over a range of collision energies E_i is shown for two different T_s in Figure 2 (Al-Halabi *et al.* 2002). The sticking probability could be fitted quite well to an exponential function of E_i , *i.e.*, $P_s = \alpha \exp(-E_i/\beta)$, with $\beta = 175$ K (here and in Fig. 2, K is used as a unit of energy, $1 \text{ K} = 8.31 \text{ J mol}^{-1}$). The values extracted for α were 1.5 for $T_s = 10$ K and 0.85 for $T_s = 70$ K (the fit for $T_s=10$ K is not valid at collision energies significantly lower than 100 K). The strong dependence of α on T_s illustrates the strong dependence of the sticking probability on T_s for H. As a result of its weak interaction with the surface, the H atom is sensitive to the fact that the water molecules are more dynamic and less packed in the warmer surface. As a result, it is more likely that an upward moving water molecule imparts momentum to the impinging H atom, and that the interaction of H with the surface is further weakened because it interacts with fewer water molecules, at higher T_s .

In Figure 2, the results for ice Ih are also compared with results of computational studies for ice I_a that used the same H-H₂O potential, so that differences should in principle be due to differences between ice Ih and ice I_a. For $T_s = 10$ K, the results for ice Ih fall between the results of ice I_a of Buch & Zhang (1991) and of Masuda *et al.* (1998). The discrepancy with the results of Masuda *et al.* is due to the use of an

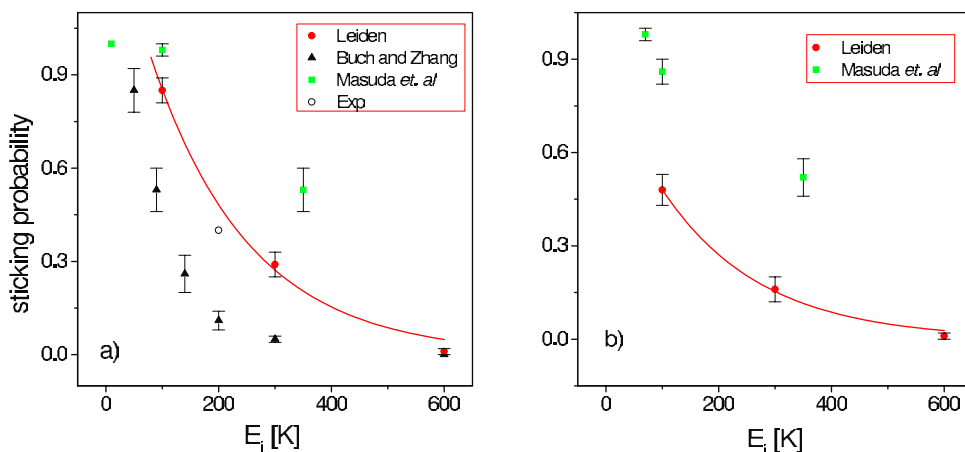


Figure 2. The sticking probability of hydrogen atoms to ice Ih is shown as a function of the collision energy E_i for (a) $T_s = 10$ K and (b) $T_s = 70$ K (Al-Halabi *et al.* 2002), together with previous computational results on sticking of hydrogen to ice I_a (Buch & Zhang 1991; Masuda *et al.* 1998). A sticking probability extracted by modeling from a TPD experiment using a 200 K atomic hydrogen beam impinging on an amorphous ice surface at low T_s is also shown (Manicó *et al.* 2001).

erroneous expression of the spherical harmonic, Y_{00} , in the equation describing the H-H₂O pair potential (Takahashi, private comm.) This expression was printed incorrectly in several papers using the H-H₂O interaction potential (Buch & Zhang 1991; Zhang *et al.* 1991).

The differences between the sticking probability for ice Ih and ice I_a computed by Buch & Zhang (1991) is probably due to differences in regularity of the ice surfaces. The amorphous ice cluster studied by Buch & Zhang is a small cluster consisting of 115 molecules. It was made by successively raining water molecules on to a small nucleus, and the surface of the cluster is quite irregular, with many sites where the impinging H may experience a significant attractive interaction to only a few water molecules. In contrast, the surface of crystalline ice (Fig. 1a) is quite regular, so that the impinging H atom can experience a significant attractive interaction with as many as six H₂O molecules, if it hits the center of a hexagonal ring. As a result of the stronger interaction, H exhibits a larger sticking probability on ice Ih than on the ice I_a modeled by Buch & Zhang. The large difference between trapping of H on ice Ih and on ice I_a here observed shows how importantly the ice structure may affect processes that are crucial to astrochemistry: after all, trapping of H on ice is important to the formation of molecular hydrogen, which is the most abundant molecule in the ISM, in dense clouds.

The difference we found between sticking of H on ice Ih and ice I_a also illustrates another important point: it is important to determine how the structure of interstellar amorphous ice is related to the conditions under which it is grown. It is believed that interstellar ice originates from chemical reactions between H and O on dust grains; as a result, the surface structure of the ice may be different than obtained by successively raining water molecules onto a pre-existing water nucleus, which could be an appropriate procedure for simulating vapor deposition of H₂O on ice.

The sticking probability we computed for $T_s = 10$ K is in good agreement with the sticking probability extracted by modeling thermal desorption experiments on sticking of H and D to amorphous ice, using a 200 K atomic hydrogen beam (Manicó *et al.* 2001). In the analysis of the experiments, the recombination efficiency γ measured was defined

through $\gamma = P_s \eta$, and the assumption was made that the recombination probability η can be taken as one, so that $P_s = \gamma$. The resulting P_s for ice I_a is in good agreement with the theory for ice Ih. Of course, this is not consistent with the difference between the theoretical results for ice Ih and ice I_a as modeled by Buch & Zhang, *i.e.*, the experimental result for P_s on ice I_a significantly differs from the theoretical results of Buch & Zhang (1991). An open question is whether the agreement between theory and experiment for ice I_a will improve if the ice I_a is set up in a different way.

3.2. CO + Ice

The P_s of CO to ice Ih and ice I_a is plotted as a function of E_i in Figure 3, for $T_s = 90$ K (Al-Halabi, van Dishoeck, & Kroes 2004). The computed P_s can be fitted quite well to an exponential function of E_i , with $\alpha = 1$ and $\beta = 90 \text{ kJ mol}^{-1}$, respectively, for both ice Ih and ice I_a. Interestingly, for CO the trapping probability appears to be the same for ice Ih and ice I_a. To within the statistical uncertainty implied by the number of classical trajectories run (100 for each energy), the probabilities are the same. In this respect, the trapping of CO to ice is different from the trapping of H to ice (Figure 2, § 3.1). At present, it is unclear whether this difference is due to the difference in the collider, or to the differences in the ice I_a model used in the calculations. In the calculations on H + ice I_a the ice I_a is modeled as a cluster of H₂O molecules successively rained on to a pre-existing H₂O nucleus (Buch & Zhang 1991), while the ice I_a used in CO + ice was obtained by rapid quenching of liquid water simulated at room temperature (Al-Halabi, van Dishoeck, & Kroes 2004).

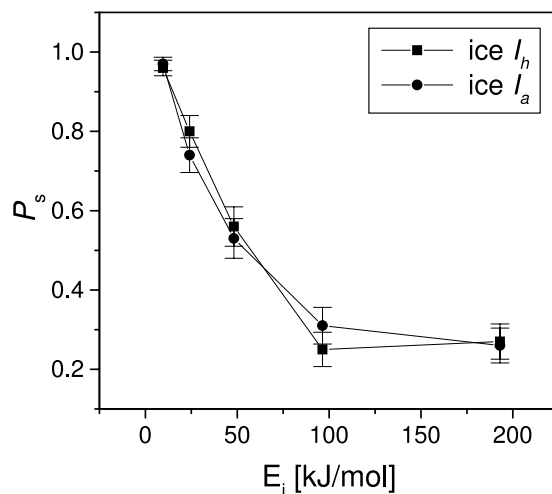


Figure 3. The P_s of CO to ice Ih and ice I_a is shown as a function of E_i , for scattering at normal incidence, and $T_s = 90$ K (Al-Halabi, van Dishoeck, & Kroes 2004).

For CO + ice, substantial P_s values were obtained for E_i (200 kJ mol⁻¹), much larger than the average adsorption of CO to ice, which is about 10 kJ mol⁻¹. This is because the energy with which the collider hits the surface can be very rapidly and efficiently dissipated through the hydrogen bonding network of ice, as also found in previous calculations on sticking of HCl to ice (Al-Halabi *et al.* 1999; Al-Halabi *et al.* 2001). In no case was a water molecule found to desorb from the surface, even though the highest E_i used was much higher than the energy with which surface water molecules are bound to the bulk of H₂O. An interesting question is whether MD simulations on sticking of atoms and molecules to CO-ice would find a similarly efficient energy dissipation and a similarly stable surface as obtained for H₂O ice.

The P_s for CO on ice is smaller than that found for HCl + ice (> 0.9 over the entire energy range depicted in Figure 3 (Al-Halabi *et al.* 1999; Al-Halabi *et al.* 2001) and effectively larger than that found for H + ice: the P_s of CO exceeds 0.8 at a value of E_i (10 kJ mol⁻¹) which is twice as large as the one (600 K \approx 5 kJ mol⁻¹) where the trapping probability of H on ice is less than 0.1 (Fig. 2). This order in the efficiency of trapping reflects the interaction strength with the surface, which is correlated to the collider-H₂O pair interaction (Table 1): the stronger the interaction with the surface, the smaller the part of the sum of the incidence energy and the interaction energy that has to be transferred from incident motion to other motions, for trapping to occur. Therefore, the larger the interaction energy with the surface is, the larger the trapping probability is, for the neutral atoms and molecules we have studied (Al-Halabi *et al.* 2002; Al-Halabi *et al.* 2003; Al-Halabi, van Dishoeck, & Kroes 2004; Al-Halabi *et al.* 1999; Al-Halabi *et al.* 2001).

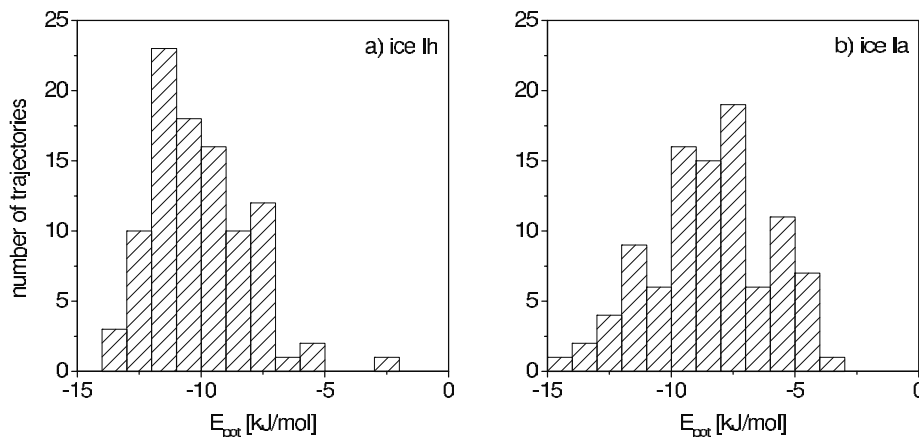


Figure 4. Using histograms, the number of sticking trajectories is shown as a function of the final value of the potential interaction energy of CO with ice, for $E_i = 9.6$ kJ mol⁻¹ and $T_s = 90$ K, for the case of ice Ih (a) and ice I_a (b) (Al-Halabi, van Dishoeck, & Kroes 2004).

From the MD simulations, it is also possible to compute the final potential interaction energy of the collider (CO) with the surface. Distributions of the adsorption energy (E_{ad}) are shown in Figure 4 for ice Ih and ice I_a (Al-Halabi, van Dishoeck, & Kroes 2004). The distribution is broader for ice I_a than for ice Ih. This reflects the greater variety of adsorption sites on ice I_a: the weakest interactions are due to CO interacting with just a few H₂O molecules protruding from the irregular surface, and similarly strong interactions can result from CO interacting with many water molecules, as can happen when CO moves into a hole in the irregular surface of ice I_a (Fig. 1d). The average adsorption energies extracted from the distributions differ somewhat; *i.e.*, E_{ad} computed for ice I_a was -8.4 ± 0.24 kJ mol⁻¹, in reasonably good agreement with the result (about 10 kJ mol⁻¹) of CO + ice I_a FT-IR experiments (Allouche *et al.* 1998; Manca *et al.* 2000; Martin *et al.* 2002), and E_{ad} computed for ice Ih was -10.1 ± 0.20 kJ mol⁻¹.

The adsorption geometry of CO on ice I_a has also been considered (Al-Halabi *et al.* 2004), in geometry optimisations in which the ice configuration (from an MD simulation) was kept fixed. The calculations suggest that CO interacts most strongly with dangling OH's (Figs. 5a and 5b), and more weakly with the bonded OH's (Figs. 5c–5e). This is in agreement with IR experiments which find the signal attributed to the interaction with dangling OH, which is observed at 2152 cm⁻¹, to be particularly strong in case of other

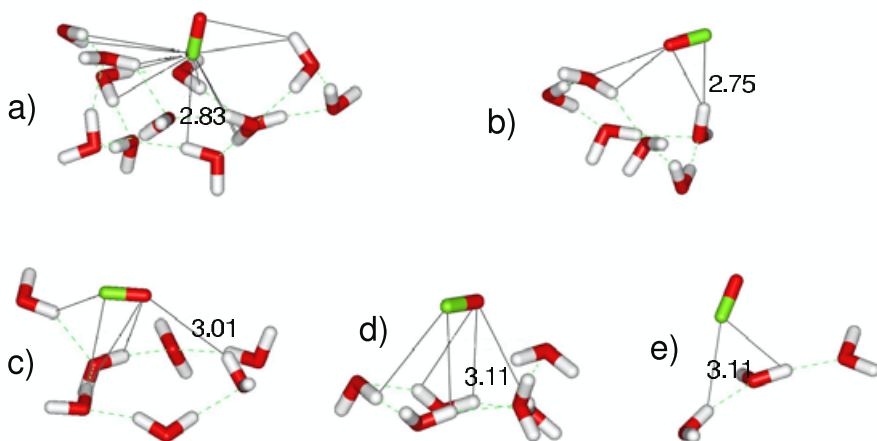


Figure 5. Examples of CO-static ice I_a configurations obtained from geometry optimisations (Al-Halabi *et al.* 2004). The five examples correspond to five different values of the potential interaction energy of CO with ice I_a, *i.e.*, (a) -0.155, (b) -0.129, (c) -0.111, (d) -0.090, and (e) -0.067 eV. Dotted lines illustrate hydrogen bonds between surface water molecules. Solid lines connect CO with the H-atoms of neighbouring water molecules that are closer to CO than 3.5 Å, the shortest H-CO distance being given in Å. Black cylinders represent O atoms, grey cylinders the C atom, and light grey spheres the H atoms. Bonding of CO to dangling OH bonds is seen in (a) and (b), while CO bonds more to “bonded OH” in (c), (d), and (e).

molecules co-adsorbed at the centres of the hexagonal rings (Devlin 1992; Martin *et al.* 2002), and absent in case of other molecules co-adsorbed at the dangling OH bonds (Devlin 1992). The absence of the 2152 cm⁻¹ feature in astronomical spectra (Pontoppidan *et al.* 2003) otherwise clearly showing the presence of CO can be used as evidence that most of the CO is not present in intimately mixed CO-H₂O ice (Pontoppidan *et al.* 2003).

3.3. $H^+ + Ice$

The P_s computed (Cabrera Sanfelix *et al.* 2005) for $H^+ +$ ice Ih is shown as a function of E_i in Figure 6 for collisions at normal incidence, at $T_s = 80$ K. The figure shows a surprising result: for low E_i ($= 0.2$ eV), P_s is significantly smaller than 1, and also significantly smaller than P_s for HCl, which exceeds 0.9 for these low E_i (Al-Halabi *et al.* 1999; Al-Halabi *et al.* 2001). This is surprising because the proton’s interaction energy with the ice surface (computed to be about 10 eV on average (Cabrera Sanfelix *et al.* 2005) is much larger (by about a factor 50) than the interaction energy of HCl with ice (Al-Halabi *et al.* 1999; Al-Halabi *et al.* 2001). The explanation for the significant reflection (40% at $E_i = 0.05$ eV) is that in the surface monolayer of ice Ih 50% of the water molecules have an electropositively charged H atom pointing away from the surface. The impinging proton experiences electrostatic repulsion when impacting close to these molecules, causing it to be reflected at low E_i . The calculations show that the rule observed for collisions of neutrals with ice (the larger the E_{ad} of the collider on ice, the larger the trapping probability) does not hold when comparing trapping of neutrals with trapping of ions.

The calculations on $H^+ +$ ice Ih also yielded another interesting prediction (Cabrera Sanfelix *et al.* 2005). Figure 7a shows that there is a significant probability (4–16% for E_i between 0.05 to 3 eV) that a water molecule desorbs upon impact of the proton (collision induced desorption). The water desorption is not due to “sputtering”; the desorption

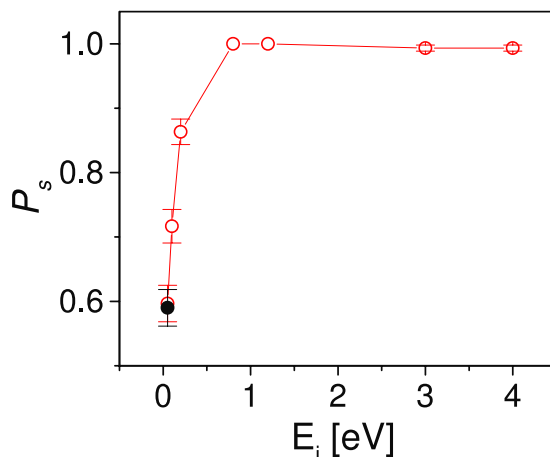


Figure 6. The sticking probability of H^+ to ice Ih is shown as a function of E_i , for normal incidence, at $T_s = 80 \text{ K}$ (open circles). The solid circle is a result of a control calculation (see Cabrera Sanfelix *et al.* 2005 for more details).

also occurs at values of E_i which are much lower (0.05 eV) than the energy with which surface H_2O molecules are bound to

the bulk of ice ($> 0.3 \text{ eV}$). Visualisation of the trajectories show that the water desorption occurs because the stuck proton disrupts the hydrogen bonding network between surface water molecules. The stuck proton can bury itself between the first and the second, or the second and the third bilayer of the ice surface (Fig. 7b). Because the proton's interaction with a neighbouring water molecule ($\approx 700 \text{ kJ mol}^{-1}$, Table 1) can be much stronger than a hydrogen bond between neighbouring water molecules ($\approx 15\text{--}20 \text{ kJ mol}^{-1}$), H^+ can act as a “Coulomb bomb” or “hydrogen bond chain saw”, completely disrupting the hydrogen bond network close to it. As a result, a nearby surface water molecule can all of a sudden find itself in a repulsive environment, and desorb.

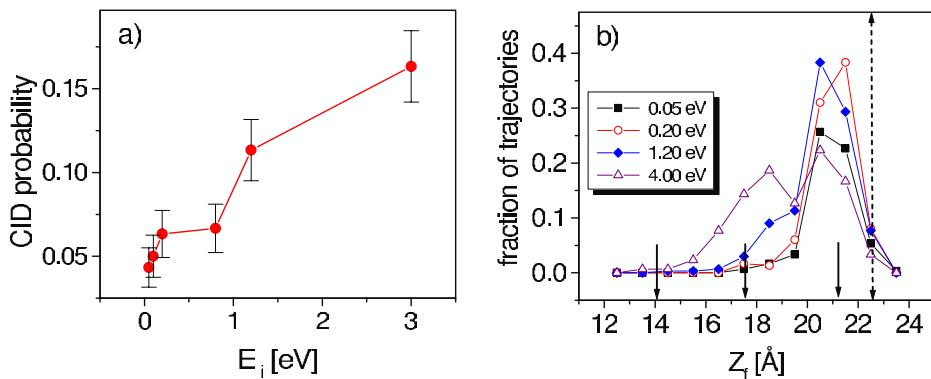


Figure 7. (a) The probability that one H_2O molecule desorbs upon impact of a proton is shown as a function of E_i , for $T_s = 80 \text{ K}$ (Cabrera Sanfelix *et al.* 2005). (b) Fraction of sticking trajectories plotted for four different E_i , according to the final value of the co-ordinate for motion normal to the surface, Z_f (Cabrera Sanfelix *et al.* 2005). The positions of the surface bilayers are shown by the arrows at the bottom of the figure. The surface-vacuum interface, indicated by the dashed long double arrow, is located at 22.5 \AA .

3.4. Photodissociation of H_2O Ice

In Figure 8 the simulated spectrum of the first absorption band of ice Ih for the old (Andersson *et al.* 2005) and new (Andersson *et al.*, in prep.) potential models are shown together with the experimental spectrum (Kobayashi 1983) and the calculated first absorption band of gas-phase H_2O . The ice spectra refer to molecules in the third bilayer, which gives a good representation of bulk spectra. The previous model gave a blueshift of 2 eV compared to the gas-phase spectrum, while the new model gives a blueshift of little over 1 eV, in good agreement with experiment (Kobayashi 1983). The experimental peak (8.6 eV) and the threshold energy (7.6 eV) are reproduced by the new potential. The calculated peaks of amorphous ice (8.6 eV) and liquid water (8.2 eV) coincide with experimental values (Kobayashi 1983; Heller *et al.* 1974). These results strongly suggest that the amount of kinetic energy released into the system is also correct.

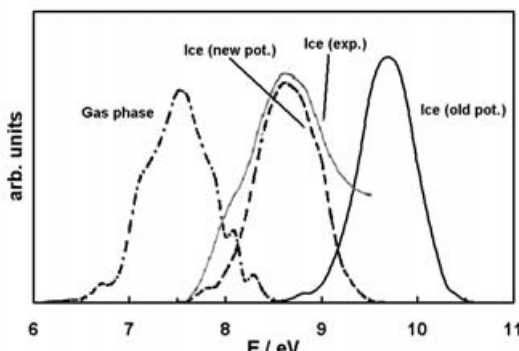


Figure 8. Simulated spectra for the first UV absorption band for ice Ih with the old (Andersson *et al.* 2005) and new (Andersson *et al.*, in prep.) potential models. Also shown are the calculated spectrum of the first band of gas-phase water UV absorption (Andersson *et al.* 2005) and the experimental spectrum for ice Ih (Kobayashi 1983).

Figure 9 shows the most important basic outcomes for ice Ih and ice I_a for photodissociation of molecules in the top three bilayers. The case where H desorbs and OH becomes trapped is the dominant outcome (60–80%) in the first bilayer. Already in the second bilayer, trapping of H and OH or of recombined water become of roughly equal importance to H atom desorption. Photodissociation in the third bilayer leads mainly to trapping of H and OH or recombined water and only in 10–15% of the cases to desorption of H. Results for the two types of ice are quite similar with a few noticeable differences. The most prominent difference is that, especially in the first two bilayers, the probability of H atom desorption is higher for ice I_a than for ice Ih (1st bilayer: 80% *vs.* 65%; 2nd bilayer: 40% *vs.* 25%). This is explained by the low density of the first bilayer in ice I_a , due to its irregular structure. H atoms moving towards the surface therefore experience fewer collisions in ice I_a than in ice Ih and have a higher probability of making it into the gas phase.

The H atoms that become trapped have on average moved about 10 Å from their original position, but atoms travelling over 60 Å have been observed. The trapped OH radicals on average only move 1–2 Å, but in cases where the photodissociation occurs at the surface, the OH has been found to move much longer distances (up to 85 Å). This is further than what is found for H atoms moving over the surface and can be explained by the OH-ice interaction being much stronger than the H-ice interaction. While H atoms moving at the surface have a high probability of desorbing, the more strongly bound OH can in most cases not desorb, but it can keep moving parallel to the surface.

Desorption of recombined water molecules is found in 0.2% of the cases for both types of ice. Indirect water desorption, where one of the molecules not initially photodissociated desorbs, has a probability of 0.2% for ice Ih and 0.04% for ice I_a . Note that these

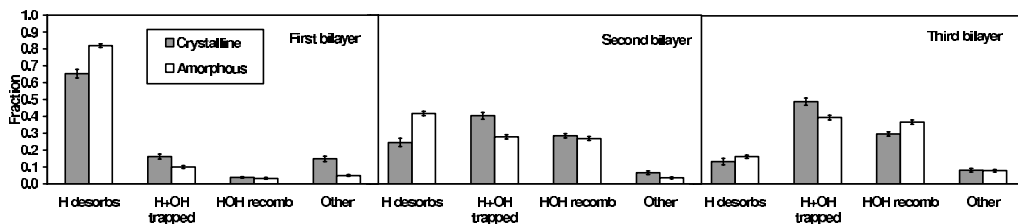


Figure 9. Probabilities (per absorbed UV photon) for the most important basic outcomes of photodissociation of water molecules in the top three bilayers in ice Ih and I_a (using the new potential model (Andersson *et al.*, in prep.). “H desorbs” is when H desorbs and OH remains trapped, “H+OH trapped” is when H and OH become trapped, and “HOH recomb” contains the cases where a recombined water molecule remains trapped. “Other” contains all other outcomes (Andersson *et al.*, in prep.)

probabilities are per absorbed UV photon. The mechanism behind this desorption is through the transfer of momentum of an energetic H atom to a water molecule, which either desorbs or initiates a further chain of momentum transfer until a molecule at the surface desorbs. The photodesorption of water is found to be quite small, but, in apparent contradiction to our results, Westley *et al.* (1995) did not detect *any* desorption of water at low temperatures ($T \leq 50$ K) in the limit of single-photon absorption. They however used Lyman- α (10.2 eV) photons, which probably leads to a different excited state than the lower excitation energies considered by us.

4. Conclusions

We have discussed MD calculations on sticking of atomic hydrogen, CO, and H^+ to ice Ih and ice I_a ; results for HCl + ice were also briefly mentioned. A general rule that emerged for sticking/trapping of neutrals to ice is that P_s increases with the adsorption energy of the collider on ice. This rule does not hold when the sticking of neutrals and ions is compared. For H and CO, we found that, for normal incidence, the computed sticking probability could be fitted quite well to an exponential function of the collision energy.

For H and CO, it was possible to compare sticking probabilities computed for interaction with ice Ih and ice I_a , in calculations using identical pair potentials for the interaction of the collider with the ice. For CO, only a small difference was found between sticking on ice Ih and ice I_a ; for H, the difference was much greater. At present, it is unclear whether this discrepancy is due to differences between the colliders, or to the different ways in which the simulated ice I_a was prepared. The observed discrepancy underlines the need for understanding how the structure of interstellar ice is related to the way it comes about in the ISM, which is a fundamental question of high importance to astrochemistry: water (mostly in ice) is the third abundant molecule in the ISM, and in dense clouds ice surfaces effectively serve as the factory for producing molecular hydrogen, which is the most abundant molecule in the ISM.

Calculations on collisions of neutrals with ice surfaces never show water desorption, even for E_i (2 eV) which significantly exceed the binding energies of surface water molecules (a few tenth's of an eV). In contrast, calculations here presented show collision induced desorption of water molecules upon impact of protons even at E_i (0.05 eV) much smaller than the binding energies of surface water molecules. In the mechanism, the proton, the interaction of which with a neighbouring water molecule can be much stronger

than a hydrogen bond between neighbouring water molecules, disrupts the hydrogen bonding network, acting like a “Coulomb bomb”.

We have also presented results of new calculations on photodissociation of water in ice Ih and ice I_a, in the first absorption band. The emphasis was on the dynamical outcome of photoexcitation of a water molecule in the top 10 Å of the ice surface (first 3 bilayers), because photoinitiated chemistry with co-adsorbed molecules, which we are interested in studying next, is most likely to occur at the surface. By adjusting the dipole moment on the excited water molecule, which affects the interaction of that water molecule with the surrounding water molecules, it was possible to reproduce the position and the shape of the first absorption band in the experimental spectrum in a semi-classical calculation.

Subsequent MD calculations show that the most important dynamical outcomes following photoexcitation in the top surface layer are dissociation followed by H-atom desorption (dominant following photoexcitation in the top bilayer) and dissociation followed by trapping of both the H and OH photofragments (dominant following photoexcitation in the third bilayer). In contrast, water desorption was found to be a very unlikely outcome (< 0.5%). The dynamics is usually complete in around 1 ps, which is much shorter than the average time-interval between subsequent collisions of UV photons with a typical ice-covered grain in dense clouds (about a week). While there are subtle differences between photodissociation of water in ice Ih and ice I_a, the similarities in the spectrum and the dynamical outcomes are more striking than the differences.

Acknowledgements

The authors like to thank E.F. van Dishoeck, who contributed importantly to the work here presented. We also thank A. Al-Halabi, who performed the calculations on sticking of H and CO to ice, and importantly contributed to the calculations on H⁺ + ice. We also thank A.W. Kleyn, M.C. van Hemert, H.J. Fraser, P. Cabrera Sanfelix, G.R. Darling, and S. Holloway, whose co-authorship on one or more of the papers discussed here reflects the importance of the contributions they made to the work presented here. We also thank R. van Harreveldt for help with the initial conditions for the calculations on photodissociation. The work of S. Andersson was funded by a NWO/Spinoza grant (for E.F. van Dishoeck), and a CW programme grant. The work was also funded by FOM, and through grants of computer time by the Stichting Nationale computerfaciliteiten (NCF).

References

- Al-Halabi, A., Kleyn, A.W., & Kroes, G.J. 1999, *Chem. Phys. Lett.* 307, 505
- Al-Halabi, A., Kleyn, A.W., & Kroes, G.J. 2001, *J. Chem. Phys.* 115, 482
- Al-Halabi, A., Kleyn, A.W., van Dishoeck, E.F., & Kroes, G.J. 2002, *J. Phys. Chem. B* 106, 6515
- Al-Halabi, A., Kleyn, A.W., van Hemert, M.C., van Dishoeck, E.F., & Kroes, G.J. 2003, *J. Phys. Chem. A* 107, 10615
- Al-Halabi, A., Fraser, H.J., Kroes, G.J., & Van Dishoeck, E.F. 2004, *A&A* 422, 777
- Al-Halabi, A., van Dishoeck, E.F., & Kroes, G.J. 2004, *J. Chem. Phys.* 120, 3358
- Allamandola, L.J., Sandford, S.A., & Valero, G.J. 1988, *Icarus* 76, 225
- Allen, M.P. & Tildesley, D.J. 1987, *Computer Simulations of Liquids* (Clarendon: Oxford)
- Allouche, A., Verlaque, P., & Pourcin, J. 1998, *J. Phys. Chem. B* 102, 89
- Andersson, S., Kroes, G.J., & van Dishoeck, E.F. 2005, *Chem. Phys. Lett.* 408, 415
- Andersson, S., Kroes, G.J., & van Dishoeck, E.F., in preparation
- Berendsen, H.J.C., Postma, J.P.M., van Gunsteren, V.F., Dinola, A., & Haak, J.R. 1984, *J. Chem. Phys.* 81, 3684

- Bernal, J.D. & Fowler, R.H. 1933, *J. Chem. Phys.* 1, 515
Buch, V. & Zhang, Q. 1991, *Ap. J.* 379, 647
Cabrera Sanfelix, P., Al-Halabi, A., Darling, G.R., Holloway, S., & Kroes, G.J. 2005, *J. Am. Chem. Soc.* 127, 3944
Devlin, J.P. 1992, *J. Phys. Chem.* 96, 6185
Dobbyn, A.J. & Knowles, P.J. 1997, *Mol. Phys.* 91, 1107
Dohnálek, Z., Kimmel, G.A., Ayotte, P., Smith, R.S., & Kay, B.D. 2003, *J. Chem. Phys.* 118, 364
Ehrenfreund, P. & Schutte, W.A. 2000, in *Astrochemistry: From Molecular Clouds to Planetary Systems*, eds. Y.C. Minh & E.F. van Dishoeck (ASP: San Francisco), vol. 197, p. 135
Ehrenfreund, P., Fraser, H.J., Blum, J., Cartwright, J.M.E., Garcia-Ruiz, J.M., Hadamcik, E., Levasseur-Regourd, A.C., Price, S., Prodi, F., & Sarkissian, A. 2003, *Plan. Space. Sci.* 51, 473
Gerakines, P.A., Moore, M.H., & Hudson, R.L. 2000, *A&A* 357, 793
Graham, A.P., Menzel, A., & Toennies, J.P. 1999, *J. Chem. Phys.* 111, 1169
Hagen, W., Tielens, A.G.G.M., & Greenberg, J.M. 1981, *Chem. Phys.* 56, 257
Heller, J.M., Jr., Hamm, R.N., Birkhoff, R.D., & Painter, L.R. 1974, *J. Chem. Phys.* 60, 3483
Herbst, E. 1995, *Annu. Rev. Phys. Chem.* 46, 27
Hollenbach, D. & Salpeter, E.E. 1971, *Ap. J.* 163, 155
Jorgensen, W.L., Chandrasekhar, J., Madura, J.D., Impey, R.W., & Klein, M.L. 1983, *J. Chem. Phys.* 79, 926
Karim, O.A. & Haymet, A.D.J. 1988, *J. Chem. Phys.* 89, 6889
Klein, S., Kochanski, E., & Strich, A. 1996, *Theor. Chim. Acta* 94, 75
Kobayashi, K. 1983, *J. Phys. Chem.* 87, 4317
Kobayashi, K., Kasamatsu, T., Kaneko, T., Koike, J., Oshima, T., Saito, T., Yamamoto, T., & Yanagawa, H. 1995, *Adv. Space Res.* 16, 21
Kozack, R.E. & Jordan, P.C. 1992, *J. Chem. Phys.* 96, 3131
Kroes, G.J. 1992, *Surf. Sci.* 275, 365
Maldoni, M.M., Robinson, G., Smith, R.G., Duley, W.W., & Scott, A. 1999, *MNRAS* 309, 325
Manca, C., Roubin, P., & Martin, C. 2000, *Chem. Phys. Lett.* 330, 21
Manicó, G., Raguni, G., Pironello, V., Roser, J.E., & Vidali, G. 2001, *Ap. J.* 548, L253
Martin, C., Manca, C., & Roubin, P. 2002, *Surf. Sci.* 502–503, 280
Masuda, K., Takahashi, J., & Mukai, T. 1998, *A&A* 330, 773
Mukai, T. & Schwem, G. 1981, *A&A* 95, 373
Petrenko, V.F. & Whitworth, R.W. 1999, *Physics of Ice* (University Press: Oxford)
Pontoppidan, K.M., Fraser, H.J., Dartois, E., Thi, W.F., van Dishoeck, E.F., Boogert, A.C.A., d'Hendecourt, L., Tielens, A.G.G.M., & Bisschop, S.E. 2003, *A&A* 408, 981
Porter, R.N. & Raff, L.M. 1976, in *Dynamics of Molecular Collisions, Part B*, ed. W.H. Miller (Plenum: New York), p. 1
Schinke, R. 1993, *Photodissociation Dynamics* (Cambridge University Press: Cambridge)
Takahashi, J., private communication
Tanaka, M., Nagata, T., Sato, S., Yamamoto, T. 1994, *Ap. J.* 430, 779
van Dishoeck, E.F. 1998, in *The Molecular Astrophysics of Stars and Galaxies*, eds. T.W. Hartquist & D.A. Williams (Clarendon Press: Oxford), p. 53
van Harreveld, R. & van Hemert, M.C. 2000, *J. Chem. Phys.* 112, 5777
van Harreveld, R., van Hemert, M.C., & Schatz, G.C. 2001, *J. Phys. Chem. A* 105, 11480
Watanabe, N. & Kouchi, A. 2002, *Ap. J.* 567, 651
Westley, M.S., Baragiola, R.A., Johnson, R.E., & Baratta, G.A. 1995, *Nature* 373, 405
Yaron, D., Peterson, K.I., Zolandz, D., Klemperer, W., Lovas, F.J., & Suenram, R.D. 1990, *J. Chem. Phys.* 92, 7095
Zhang, Q., Sabelli, N., & Buch, V. 1991, *J. Chem. Phys.* 95, 1080

Discussion

HERBST: What do you suspect happens when high energy ions strike crystalline and amorphous ice?

KROES: Brown *et al.* have studied scattering of high energy protons (0.5 MeV and 1.5 MeV, respectively) from amorphous ice (1978, *Phys. Rev. Lett.* 40, 1027). Their most important finding was that the sputtering yield (number of water molecules sputtered per incident ion) was 0.4 for a collision energy of 0.5 MeV, and 0.2 for 1.5 MeV. Extrapolating to the most usual energies of cosmic rays (approximately 100 MeV), one would think that at such high incidence energies no sputtering would be observed at all. I know of no experiments that have been done at these high energies. A recent review discussing sputtering of ice by highly energetic positive ions is that of Baragiola *et al.* (2003, *Nucl. Instrum. Methods Phys. Res. B* 209, 294), who mention that the experiments of Brown *et al.* (at 0.5 and 1.5 MeV) suggest that sputtering is an important phenomenon on icy satellites and grains subject to irradiation by energetic ions from solar flares and by magnetospheric ions.